MBS TECHNICAL REPORT 16-04

Investigating Potential Human Tetrachromacy in Individuals with Tetrachromat Genotypes Using Multispectral Techniques

Vladimir A. Bochko, Department of Electrical Engineering and Energy Technology, University of Vaasa, FIN-65101 Vaasa, Finland;
Kimberly A. Jameson, Institute for Mathematical Behavioral Sciences, University of California, Irvine, CA, USA

Abstract

This article uses multispectral techniques to investigate color processing in two individuals possessing photopigment genotypes allowing potential human tetrachromacy. In our investigations we measure spectral reflectances from empirically reproduced color sensations of potential tetrachromat observers, and investigate color processing basis functions underlying the observed set of tetrachromat spectra. Our investigations provide new empirical and quantitative methods for estimating trichromat individuals personalized spectral sensitivities, and, as shown in one potential tetrachromat examined, permit estimation of spectral sensitivities for cases that may not conform to the kind of standard dimensional solutions typically associated with trichromat models.

1 Introduction

Conventional color technologies — such as digital cameras, computer displays and television systems — are typically based on three display primaries or filters, and are thus inherently constrained by device-dependent metamerism in the reproduction of high quality color images. Constraints on high quality color reproduction that arise from device-dependent metamerism occur when a device's display primaries (or filters) do not provide adequate gamut or intensity ranges to approximate those typical of the human color vision system. When such limitations exist, subtle color appearance variations that may be apparent to a human observer engaged in naturalistic viewing of a scene, can be lost when an image of that scene is reproduced on a display device.

Historically display engineers have addressed device-dependent metamerism by identifying sets of primaries that best accommodate human visual system sensitivities and variations. While three-color-channel systems have long been considered standard, advances in digital display and camera industries now make it both technologically possible and economically feasible to consider extending device primaries beyond the three typically used.

The present article investigates (a) potential image reproduction enhancements made possible by extending the number of display primaries of a color system, and (b) what such advances might imply for not only observers with normal color vision, but also for observers with exceptional color vision owing to color vision photoreceptor processing that potentially confers richer color experience. Here we describe how analyses of *potential tetrachromat color vision* can lend insight into effectively addressing the device-dependent metamerism problem, as well as suggest how to generally enhance color representation in digital imaging technology. In addition, results show that studying color vision in potential tetrachromat observers clarifies some color vision features associated with four-photoreceptor color vision phenotypes, which may aid in extending display technologies towards multispectral imaging systems.

Potential Human Tetrachromacy

Potential human tetrachromacy is a recently noted form of human color perception [23], made possible by inheritance of altered X-chromosome-linked photopigment opsin genes responsible for human color vision. Potential tetrachromat individuals carry gene sequences that permit expression of four distinct classes of daylight-sensitive retinal photoreceptors used for visual processing environmental color stimuli. Individuals with retinas expressing a tetrachromat potential differ from the majority of people who typically possess genes for three distinct photopigmet opsins, and who, as a result, retinally express up to three classes of daylight photosensitive cells. The latter configuration is analogous to that engineered in standard three-primary display devices, and models with three distinct classes of photoreceptors, which, when neurally represented as a trivariant color code, have long been accepted as the standard for normal human color vision and widely considered the basis for typical ranges of normal perceived color appearance.

Genetic variations most often linked to human potential tetrachromacy derive from individual's X-chromosome-linked photopigment opsin genes. Genetic variants, or opsin sequence *alleles*, of standard medium-wavelength and long-wavelength sensitive photoreceptors ("M-cone" and "L-cone", respectively) provide sequence variations that make tetrachromacy possible. Females with two X-chromosomes are capable of retinal expression of four different wavelength-sensitive photoreceptor classes (S-, M-, L- plus a distinct alternative, presumably a variant of the usual L-cone class, often referred to as L'-, or *L-prime*) making them "retinal tetrachromats", while males with a full complement of X-linked opsin genotype on their single X-chromosome are presumed to express some form of three different wavelength-sensitive photoreceptor classes, conferring such males with color vision trichromacy.

Since the 1980's empirical results have emerged suggesting that retinal tetrachromacy may provide a photopic

response that allows observers to distinguish more colors than that experienced by conventional trichromat color vision. [22–24]. Individuals genotyped as having a potential for tetrachromacy have since been empirically investigated by several different groups, with the general result being that some potential tetrachromats experience non-deficient color vision, which, in some cases, seems *better than normal*, and is not fully captured by a normal model of trichromat color vision (see [4, 11–13, 17, 18, 25]). Recent empirical investigations compare one specific potential tetrachromat individual (CA) to other control participants and finds empirical results suggesting observer CA, (i) sees more colors under conditions of dim illumination (especially for stimuli having dominant wavelengths coincident with the putative peak of her extra photopigment's sensitivity response), and (ii) essentially judges some appearances as "colorful" that a normal trichromat observer performance suggests are relatively colorless appearances. [15, 16] In general, potential tetrachromat CA's results suggest a psychophysical transformation reflecting non-uniform variation compared to a normal observer's performance – that is, it included regions of deviation from normal for some color stimuli, while other color space regions showed CA's processing was indistinguishable from normal processing. [15, 16]

The present article empirically explores the potential perceptual consequences of retinal tetrachromacy through investigations of color perception and the modeling of color processing behaviors using multispectral analysis techniques. Owing to their general utility and efficiency in data inspection, we employ machine learning algorithms to investigate color processing underlying the observed phenomena: That is, estimating optimal color matching functions from tetrachromat behavioral data.

To address this problem we could estimate observer's spectral basis functions based on empirical observations using principal component analysis (PCA) methods. However, due to dimensional orthogonality in the present case, PCA basis function solutions of these data are likely to contain negative coefficients that make physical implementation problematic. An appropriate alternative is Non-negative Matrix Factorization (NMF) or Non-negative Tensor Factorization (NTF) which may provide useful non-negative decompositions of these data. Thus, NMF and NTF are used to define the optimal non-negative representation of spectral colors for data from different sets of stimuli, including the Macbeth ColorChecker (MCC), a Munsell spectral color set and paint spectral sets [1, 5, 19].

As described below we present two independent studies. First, we collect empirical observations for two observers' color perception variations of a standardized color stimulus. And, second, we employ the NMF genetic algorithm to calculate approximate basis functions for spectra associated with a tetrachromatic color vision model.

We implement two algorithms to calculate the basis functions. The first algorithm finds basis functions by minimizing mean–squared errors between given spectra and their approximations and works in spectral space. The second algorithm finds basis functions minimizing color differences when spectra and spectral approximations are converted to colors. The second algorithm provides optimizations in color space. For conversion we use a three channel algorithm which is used for reproduction colors from spectra [7]. While the first algorithm solves the task in an appropriate way, the second algorithm may over specify its solutions by assuming three–channel color reproduction for tetrachromatic data. Despite this potential limitation, results suggest that it is reasonable to accept three–channel color reproduction from simulated tetrachromatic spectral reflectance. We consider such reproductions as mappings to a three–dimensional space that provides valuable characteristics of calculated basis functions. Three channel reproduction helps to obtain the smoother and better localized basis functions that cannot be achieved with methods working in spectral space. In addition, the experiments with three–channel system indicate significant improvement in color reproduction compared to spectral optimization. This was established in our previous study with three channel systems [5]. Therefore, as described below, results obtained suggests that the three–channel color reproduction method in color space is useful for understanding some potential tetrachromat color perception differences explored in the present study.

The paper is arranged as follows: Color vision models based on empirically observed color perception behaviors are considered in Section 2, empirical methods for collecting tetrachromat spectral reflectance stimuli are described in Section 3, data dimensionality and basis function calculation are explained in Section 4, experimental results are given in Section 5, and conclusions are given in Section 6.

2 Two color vision models

Color vision models provide a principled basis for understanding human color perception. In modeling developed here we first consider a trichromat color vision model [10]. We assume that the composition of the spectral power $E(\lambda)$ of an illuminant and the spectral reflectance $s(\lambda)$ of an object are sufficient to physically characterize subjective color of a spectral stimulus $\varphi(\lambda)$. The Standard Observer senses these physical stimulus values and integrates them to provide spectral color stimuli using three color matching functions: $\overline{x}(\lambda)$, $\overline{y}(\lambda)$ and $\overline{z}(\lambda)$. The result of the integration can be described as tristimulus values which specify color sensations (Fig. 1) for a trichromat observer as X, Y, and Z. [29]

Similarly, initial color vision processing in a retinal tetrachromat can be characterized by altering the underlying color matching functions, varying their number, shape and wavelength range. In such cases, tetrachromat processing can be denoted as $\bar{t}_l(\lambda)$, $\bar{t}_{ml}(\lambda)$, $\bar{t}_m(\lambda)$ and $\bar{t}_s(\lambda)$ corresponding to the long, middle-long, middle and short subrange of wavelengths. Tetrastimulus values T_l, T_{ml}, T_m, and T_s thus depend on the integration of the product of four color matching functions and color stimulus spectra (Fig. 1). The tetrastimulus values provide a basis for color sensations arising from tetrachromat retinae. Thus, the two color vision models presented provide formal descriptions for color sensation variations occurring in a standard observer compared to a tetrachromat observer.

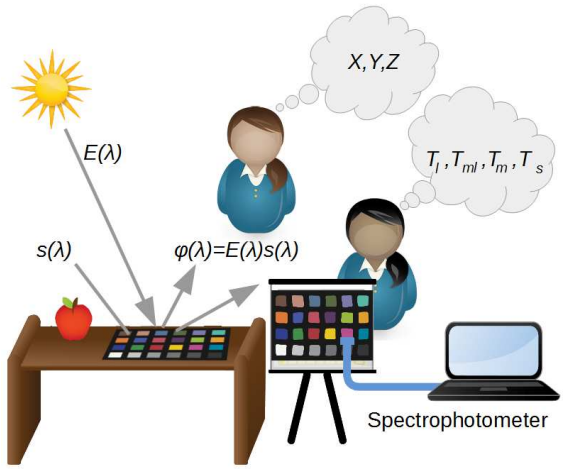

Figure 1. *Two color vision models based on tristimulus and tetrastimulus values.*

An important component for understanding tetrachromat color perception is the accurate estimation of tetrachromat color matching functions, or chromatic response functions that arise from the initial limiting constraints found in cone spectral sensitivity variants. Previous research suggests how cone fundamentals can be simulated for a potential tetrachromat [18]. By comparison, here we simulate cone fundamentals using a machine learning algorithm which provides approximations of the color matching functions underlying observed color perception behavior, and represents a new engineering approach for studying the perceptual consequences of retinal tetrachomat color vision processing.

3 Color Reproduction Experiment

The analytic methods developed in Section 4 make use of personalized color perception variation that is assessed through empirically observed color reproduction.

3.1 Participants

As shown in previous photopigment opsin genotyping research molecular genetics research has determined that genotypes involving more than three normal photopigment opsin variants are not uncommon, [3, 4, 12, 13, 18, 25] and it is thought that mechanisms governing expression of such photopigment opsin genes does not rule out the possibility that an individual will express more than three classes of retinal photopigments. The aim of much of the research into potential human tetrachromacy has been to discover (a) how the possession of extra photopigment opsin genes may alter perceptual processing of color, and (b) what the X-chromosome linked features of the L-cone and M-cone opsin genes implies for potential human tetrachromacy and gender-linked color vision processing differences. [14]

Here we describe color perception assessment of two observers. The first individual is female participant "CA" with superior (non-deficient) color perception, who, prior to the present study, was genetically confirmed as possessing a potential tetrachromat genotype. [15, 16] The second participant is female participant "LG," also assessed as having superior (non-deficient) color perception, and whose photopigment opsin genotype was unknown prior to the color perception assessment presented next in section 3.2, but who was considered to be appropriate as a trichromat control participant. Surprisingly, however, subsequent to collection of the present behavioral data, participant "LG" was genetically assessed and found to possess a potential tetrachromat genotype. [16] Thus, in the present investigations, two participants with genotypes for potential retinal tetrachromacy are compared.

In addition to being genotyped as potential tetrachromats, CA and LG both have (*i*) a life history of art education, training and practice; and (*ii*) have accomplished portfolios as oil painters that include art works on diverse ranges of naturalistic objects and scenes, and have sold and/or exhibited their paintings for profit. Thus, both participants are confirmed as having a genetic potential for color vision tetrachromacy, have extensive color perception learning experience through art education and practice, and have excellent art skills.

As previously reported [15,16], CA and LG volunteered for participation in a series of investigations involving color perception for which participants' opsin DNA sequences were genotyped using a novel implementation of polymerase chain-reaction (PCR) methods. [2, 12, 26] All genotyping was performed with participants' informed written consent using procedures that adhere to protocols compliant with the world medical association declaration of Helsinki ethical principles for research involving human subjects, and were approved by the ethical review board of the University of California, Irvine. Figure 2 shows the L-opsin Exon 3 Ser-180-Ala genetic sequence excerpts for the two participants discussed here.

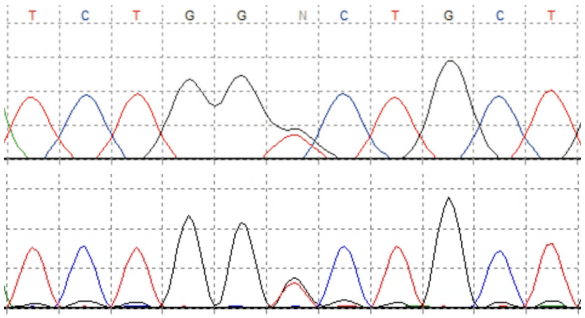

Figure 2. *Genetic sequence detail of the L-opsin gene for two different potential tetrachromat participants. Top panel depicts an excerpt of the L-opsin gene sequence for CA, and the bottom panel shows the corresponding sequence for LG. Curved peaks depict the intensity of the nucleotides (ddNTPs) observed in the DNA. For both participants column 6 of the sequences show L-opsin Exon 3 codon 180 loci where two allelic variants – corresponding to serine and alanine – are apparent.*

3.2 Methods

Subjects and Design. Phase 1 involved 1-2 hours of testing to assess color vision using standardized methods. Phase 2 involved collecting self-paced painted color samples from participants. Total approximate duration of ex-

perimental participation during a single session was between 4 and 4.5 hours. All behavioral investigations were performed with participants informed written consent, as approved by the ethical review board of the University of California, Irvine.

Phase 1: Participants were assessed using standardized procedures and some novel analysis approaches. Diagnostics for color deficiency used were Ishihara Pseudo-isochromatic Plates, the Farnsworth-Munsell 100-hue Test, and the O.S.C.A.R. flicker photometric test and the Neitz anomaloscope matching task. Both participants were classified on all tests as having normal color vision.

Phase 2: Following standardized color testing, both participants were assessed in a color reproduction experiment to obtain (*i*) observer-specific reproductions of the Munsell Color Checker standard stimulus [20], for evaluating observer's individual variation in color perception; and (*ii*) quantification of personalized color perception variations relative to a known standard observer model, for the purposes of designing color vision models described in Section 4 below.

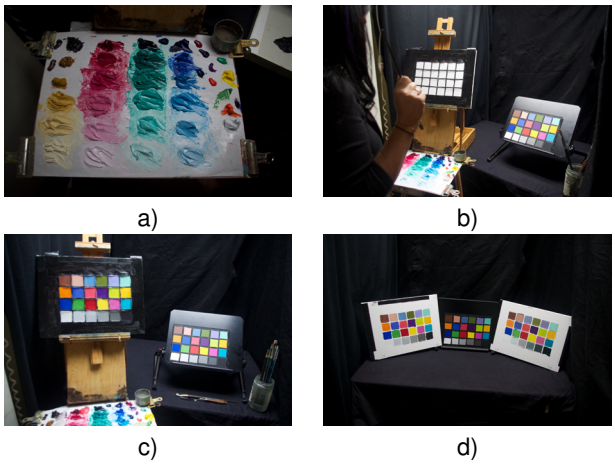

Figure 3. *Color Reproduction Experiment. Two research participants reproduced the 24 color appearances of the Munsell Color Checker. Panels shown depict a set-up that was identical across both participants' experimental sessions. Both artists a) started with identical paint pigment palettes. b) Reproduced the 24 MCC squares under the same illuminant (D65), at the same viewing distance, and in the same physical viewing booth set up. c) Were permitted as much time as needed to reproduce the 24 MCC colors, and finished when they were satisfied that their painted version faithfully reproduced the color appearances of the MCC. d) Completed the MCC reproductions in separate self–paced sessions in under 40 minutes.*

Fig. 3 depicts the empirical setting, pigment palettes used, and reproductions produced by participants CA and LG. At the start of each session a palette of agreed–upon pigments was created and two identical copies of the palette were made for use in the individual experimental sessions (see Fig. 3a). As shown in Fig. 3b, the viewing booth set up was illuminated from above by a standardized illuminant approximating a D65 illumination source using 4 lightbulbs in a fixture designed for optimal light distribution, standardized for industrial proofing and color control [9]. Lamps were warmed-up 1-hour prior to start of the experimental session and participants were adapted to the environment for a minimum of 30 minutes. During the session participants were permitted free viewing of the stimuli, the palette and a canvas (configured with a dark MCC stimulus surround overlay that outlined 24 segments, of 4 cm. square, of blank canvas to be painted), which were viewed at estimated distances of ~75 cm., ~40 cm., ~60 cm., respectively. The two participants were run under two illuminant conditions: First, for a D65 illuminant and, second, adapted under a filtered chromatic illuminant (only results from the D65 illuminant condition are reported here).

Using a color reproduction task for assessing individual variation in color perception is, admittedly, a non-standard empirical design. However, we chose it based on the pragmatic rationale that both participants (a) have advanced color training and expertise, and (b) are accomplished painters who demonstrate high-level skill at reproducing their color experiences using paints on canvas, and followed the reasoning that, to the degree that the observers could accurately reproduce the appearance of color stimuli with pigments, comparing individual differences of participants relative to a standard observer model would provide useful information on the color perception variation across the individual observers. The instructions to participants were to "take as much time as needed to *exactly duplicate* the 24 colors shown [the MCC stimulus] using the pigment palette provided, paying the utmost attention to color reproduction accuracy" ... "you may return to adjust any one of the color patches at time," before signaling to the experimenter that you have either (1) achieved an identical color match between the samples and reproductions, (2) achieved an identical, or satisfactory, color match between some samples, but not all samples (please specify which), or (3) were unable to achieve a satisfactory color match between the samples and their reproductions using the pigment palette provided.

Here we use the Macbeth ColorChecker and painted reproductions of the MCC independently produced by each potential tetrachromat participant. Paintings of MCC color patches are made under laboratory conditions at constant illumination. The observed colors of MCC and painted patches are a composition of spectral reflectance and illuminant spectral power distribution. We assume that if a trichromat model of color appearance is appropriate, then, for a given potential tetrachromat observer, if they empirically report that a painted patch visually matches an MCC patch, then the measured spectral reflectance of painted patches should have the same X, Y, Z tristimulus values as the spectral reflectance of MCC, and thereby satisfy the classical definition of metamerism. Moreover, we assume that if we observe that measured MCC and painted patch colors that have the same X, Y, Z tristimulus values appear different to a given potential tetrachromat observer, then we suppose that such differences in appearance primarily depend on features of observer perceptual processing that differ from the tristimulus model (however, see further discussion below), which therefore can be investigated using analyses of measured spectral reflectances of painted patches compared to reflectances of the MCC standard.

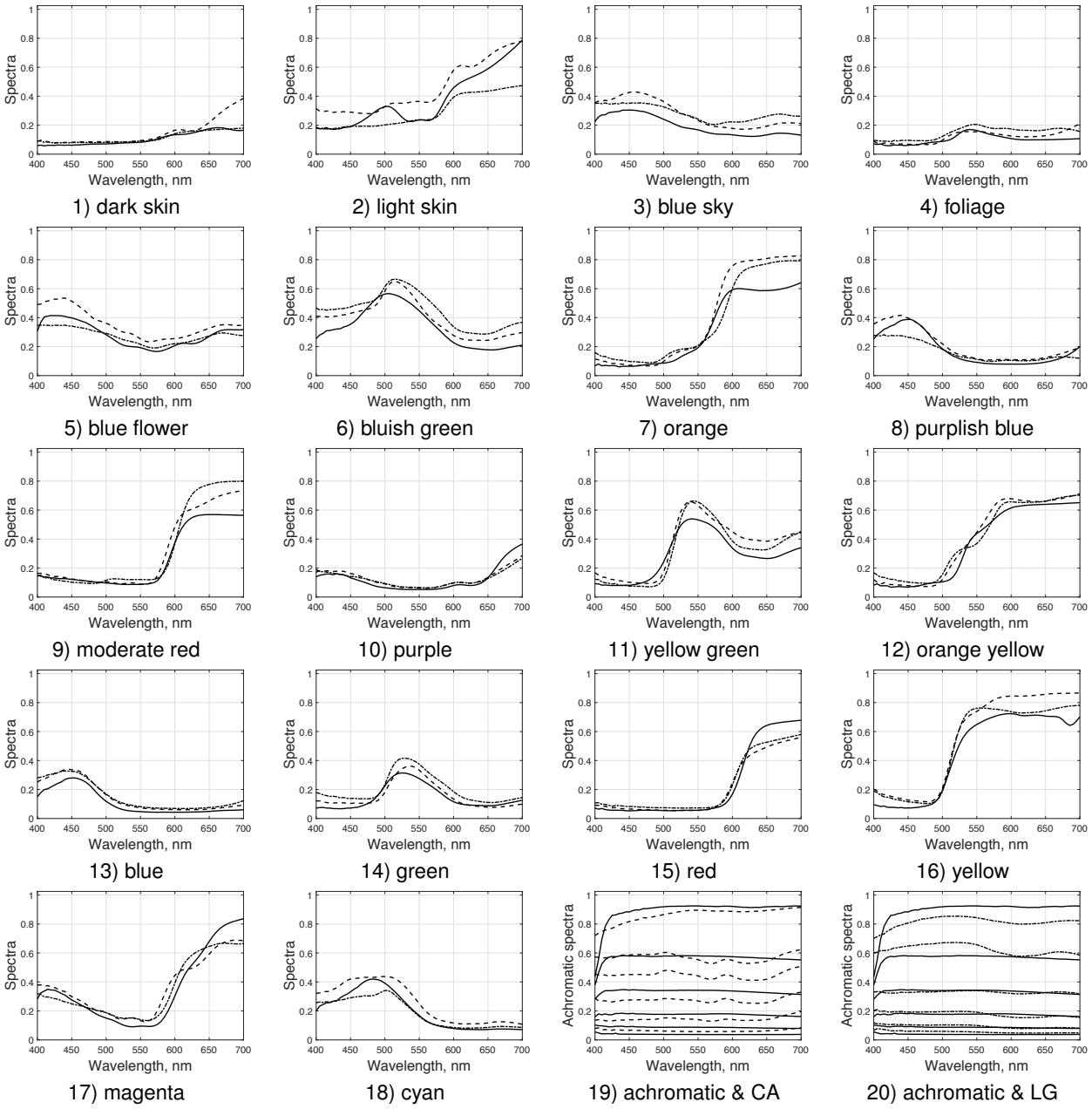

Figure 4. *MCC spectra for chromatic stimuli (panels 1-18) and for composite graphs depicting MCC curves for 6 achromatic stimuli with the corresponding participant curves (panels 19-20). Panel enumeration corresponds to the series shown in Fig. 5, such that MCC row 1 colors from left to right correspond to panels 1-6 shown here, MCC row 2 colors correspond to panels 7-12 shown, and MCC row 3 colors correspond to panels 13-18 shown. Panels 1-18 depict spectra for MCC (solid line), CA (dash line) and LG (dash dotted line). Panel 19 shows CA's spectra (dashed) compared to 6 achromatic MCC spectra. Panel 20 shows LG's spectra (dot-dashed) compared to 6 achromatic MCC spectra. Six achromatic stimuli are depicted as Fig. 5's achromatic series shown. Color nomenclature from [21]*

For modeling purposes we use spectral reflectance measures of the 24 painted reproductions of the MCC stimuli to compare with the reflectance measures of the standard MCC stimulus, which provides us with an informative database for analyzing each participant's individual color vision mechanisms. That is, because every painted color patch has particular spectral reflectance, we posit that to the degree spectral reflectance measures of painted a patch differs from spectral reflectance measures $s(\lambda)$ of a corresponding MCC patch, that difference relates to each participant's individual metameric color sensations.

Note, however, according to Foster et al., "...metamerism occurs when light with different spectra appear the same to the eye/sensor system. Metamerisms arise because the number of degrees of freedom in a sensor system — three for the cone receptors in the normal human eye or filters of a typical RGB camera — is smaller than the degrees of freedom needed to accurately represent light spectra." [8] And, in the present investigations the dimension of a sensor space could be 3 or 4, and the dimension of a spectral space is generally higher (e.g., here it equals 61, as defined in Section 5.1). Thus, here mappings from color (colored patch) to spectra (simulated spectra) are one-to-many, and observed X, Y, Z correspondences between simulated spectra and MCC spectra can be effected by at least two different sources of influence.

For example, influences may arise from, (1) perceptual experience variations attributable to tetrachromacy that provide evidence (in the form of disrupted metameric appearance equivalence relations between classically modelled pairs with equivalent tristimulus values) against a tristimulus model as appropriate for describing tetrachromat color processing. Or, (2) cases where identical appearances arising from tristimulus metamers (colors are the same but reflectance spectra are different) turn out by chance (see [8]) to be similarly metameric for a tetrachromat, thereby incorrectly providing support for a tristimulus model of tetrachromat color processing when a trichromat model is actually either inappropriate or only locally appropriate (following a possible dimensional degeneracy in some spectral region).

Based on the foregoing, we generally assume that a spectrum of a painted sample can be described as a "simulated spectrum" for that observer. An observer's set of simulated spectra can be represented by some number of basis function that accurately describes the entire set of reproduced spectra. An Ocean Optics USB 2000 spectrometer (Fig. 1) was used to measure each participant's 24 color reproductions which were compared to the know measures of the MacBeth Color Checker Classic. [20]

MCC stimulus measurements are shown in Fig. 4, and Fig. 5 shows approximations of color appearances found in the MCC standard stimulus. [21] Inspection of the measurements reveal that the spectra corresponding to yellow/green (11) and some orange/yellow colors (7, 12 and 16) are less uniform for CA and LG than MCC spectra. The manner with which they were found to vary from the MCC standard suggests that, qualitatively, participant CA and LG render the noted stimuli as more saturated as reproduced colors. The achromatic spectra for CA clearly indicate that CA has enhanced sensitivity for dark gray shades. Her spectral values for patches 21–24 are higher than MCC spectra. The LG achromatic spectra are close to MCC spectra.

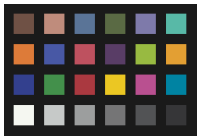

Figure 5. *Approximate colors appearances simulating the MCC standard stimulus.*

4 Data dimensionality and basis functions

Non-negative matrix factorization is used to define the optimal non-negative representation of spectral colors for each participant's simulated spectra of MCC. The NMF method represents spectra by a few non-negative basis functions. NMF determines non-negative factors $\boldsymbol{W}$ and $\boldsymbol{H}$ using non-negative factorization of the given spectral data $\boldsymbol{V}$ as follows: $\boldsymbol{V} = \boldsymbol{WH}$. The matrix size is defined as: $\boldsymbol{V} \in \mathbb{R}^{d \times n}$, $\boldsymbol{W} \in \mathbb{R}^{d \times l}$ and $\boldsymbol{H} \in \mathbb{R}^{l \times n}$, where d is the number of wavelengths, n is the number of spectral colors, and l is the number of basis functions. Thus, the columns of $\boldsymbol{W}$ are the basis functions, and $\boldsymbol{H}$ is a matrix of weights, that minimize the error of the approximation.

4.1 Data dimensionality

We define the data dimension for MCC and simulated MCC spectra. We use an ISOMAP technique which finds a low-dimensional embedding in a high-dimensional observation. For estimating data dimensionality ISOMAP is superior to methods such as Principle Component Analysis (PCA) and Multi-Dimensional Scaling (MDS) [27]. To define data dimensionality ISOMAP analyzes the data matrix $\boldsymbol{V}$ and calculates a residual variance against the number of embedded components.

The ISOMAP residual variance is defined:

$$1 - R^2(D_G, D_Y), \tag{1}$$

where R is the correlation coefficient taken over all elements of D_G and D_Y, D_Y is the matrix of Euclidean distances in the low dimensional subspace recovered by ISOMAP and D_G is the graph distance matrix of input data $\boldsymbol{V}$.

4.2 Basis functions for simulated spectra

Elsewhere we propose two NMF approaches minimizing spectral differences and color differences, both of which use a genetic algorithm (GA). [5] Bochko et al.'s first approach used spectral differences which provided results similar to standard NMF. Their second approach, however, was based on color differences and produced much more desirable results compared to the first approach based on spectra differences. In this case, the basis functions are more orthogonal and bell-shaped because their tails decay fast.

As reported previously, [5] the approach based on spectral differences utilizes an optimization method with a non-negativity constraint. The non-negative matrix factorization

solves the following objective function in spectral space:

$$\min_{\boldsymbol{W},\boldsymbol{H}} \quad \sum_{i=1}^{n} \|\boldsymbol{v}_i - \boldsymbol{W}\boldsymbol{h}_i\|^2 \quad \text{subject to } \boldsymbol{W},\boldsymbol{h}_i \geq 0, \tag{2}$$

where $\boldsymbol{v}_i$ and $\boldsymbol{h}_i$ are the columns of the matrices $\boldsymbol{V}$ and $\boldsymbol{H}$, respectively, and $\boldsymbol{W}$ and $\boldsymbol{h}_i$ have all non-negative elements.

The NMF method gives surprisingly good results when comparing MCC spectra with a model based on Standard Observer color matching functions [29] and cone fundamentals [30] (Fig. 6). Although basis functions are not color matching functions, they are positive and resemble color matching functions in shape, and they serve as limiting conditions for color matching, as well as capture operating characteristics and information about receptor class functional responses to spectral wavelengths (Fig. 6c).

By comparison, the approach based on color differences adopts an objective function in color space:

$$\min_{\boldsymbol{W},\boldsymbol{H}} \quad \sum_{i=1}^{n} \left\|\boldsymbol{f}(\boldsymbol{v}_i) - \boldsymbol{f}(\boldsymbol{W}\boldsymbol{h}_i)\right\|^2 \quad \text{subject to } \boldsymbol{W},\boldsymbol{h}_i \geq 0, \tag{3}$$

where $\boldsymbol{f}()$ is a spectrum-to-color conversion function [7]. Then $\left\|\Delta E^*_{abi}\right\|^2 = \left\|\boldsymbol{f}(\boldsymbol{v}_i) - \boldsymbol{f}(\boldsymbol{W}\boldsymbol{h}_i)\right\|^2$, where ΔE^*_{ab} is a CIELAB color difference: $\Delta E^*_{ab} = \sqrt{\left(L^*_v - L^*_{Wh}\right)^2 + \left(a^*_v - a^*_{Wh}\right)^2 + \left(b^*_v - b^*_{Wh}\right)^2}$. We denote $[L^*_v \;\; a^*_v \;\; b^*_v]^T = \boldsymbol{f}(\boldsymbol{v})$ and $[L^*_{Wh} \;\; a^*_{Wh} \;\; b^*_{Wh}]^T = \boldsymbol{f}(\boldsymbol{W}\boldsymbol{h})$. [6]

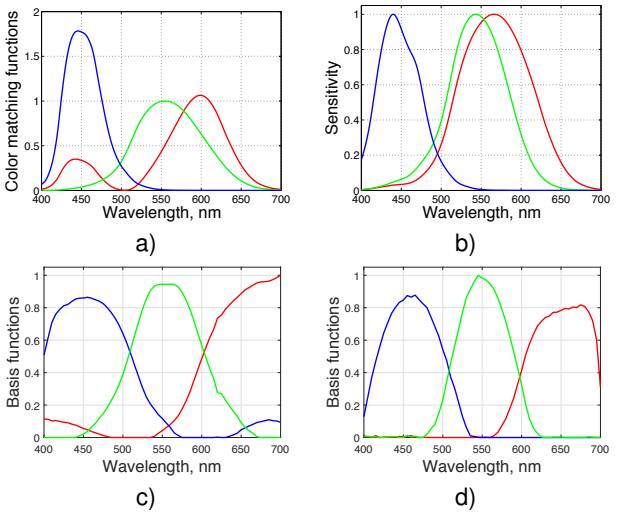

Figure 6. *Spectral curves. a) CIE 1931 color matching functions of Standard Observer. [29] b) The Smith and Pokorny (1975) cone fundamentals. [30] c) Normalized basis functions calculated using the MCC color spectra and optimized in spectral space. d) The normalized basis functions calculated using the MCC color spectra and optimized in color space.*

Fig. 6d shows that the basis functions optimized in color space are well-formed and better localized than those ones optimized in spectral space (Fig. 6d). These basis functions are much more accurate than in spectral space reducing the approximation error of spectral colors by a factor of 6 for MCC colors [5].

5 Simulation Investigations

Investigations were conducted to obtain empirically-derived basis functions from sets of simulated tetrachromat spectra.

5.1 Basis functions

Three distinct sets of basis functions were calculated for MCC and two observers (LG and CA) from simulated spectra using optimization in two spaces: spectral space and color space (Eq. 2 and Eq. 3). For simplicity, a subset of available wavelengths were employed in the range [400,700] nm, producing sets of 61 values taken at 5 nm intervals. We permitted variation in the number of basis functions in a solution. The number of the MCC spectral colors was constrained to the 24 provided in the standard (Fig. 5). Data from two potential tetrachromats described earlier, LG and CA, was measured from each participant's painted color patches using a spectrophotometer (Fig. 1). Thus, we have three spectral sets: MCC, MCC-LG and MCC-CA.

We define the data dimension for each data set. For that we use ISOMAP and plot a residual variance (Eq. 1) versus dimension (Fig. 7). The heuristic suggests to select the point where the residual variance values asymptote. ISOMAP was run with neighborhood parameter 4. ISOMAP shows that the solution obtained for the MCC-CA spectral set is higher than the others and equals a 4-dimensional solution. By comparison, the dimensional solutions observed for both MCC and MCC-LG show residual variance appears to asymptote at 3 dimensions.

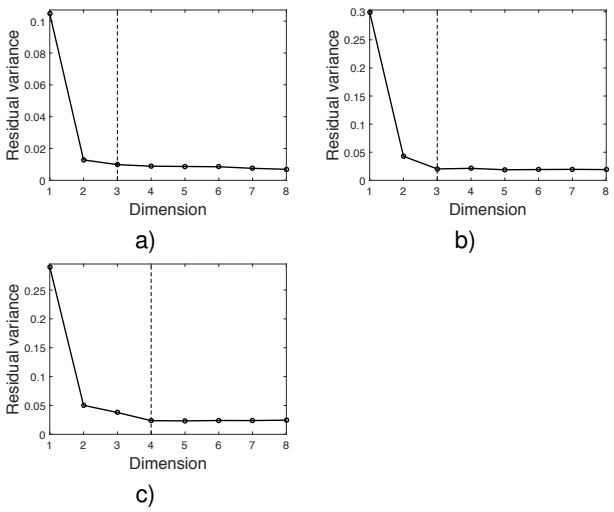

Figure 7. *Data dimension shown by a vertical dash line. a) MCC spectra. b) LG simulated spectra. c) CA simulated spectra.*

In addition, data dimensionality is taken into account in our NMF algorithm. The NMF algorithm uses Singular Value Decomposition (SVD) for initialization [28]. The SVD method uses $p+1$ leading components of SVD decomposition, where p leading components contain less than 90% of a total variance. The number $p+1$ defines the rank of factorization. For two leading components of the MCC-LG set and three leading components of MCC and MCC-CA sets the 90% threshold is not exceeded. Thus, a three ba-

sis function decomposition for MCC-LG data and four basis function decompositions for MCC and MCC-CA data are observed. For MCC-LG data increasing the variance–accounted–for threshold to 93% makes a four basis function decomposition possible as well.

While our ISOMAP and SVD analyses indicate that MCC's dimensionality is either 3 (in the ISOMAP case) or 4 (in the SVD case), for reasons elaborated below we believe the correct interpretation of these results is that a three dimensional model is appropriate for both MCC and LG spectral data sets, and that a four dimensional model is required to characterize the CA spectral data.

Note, while we interpret the above mentioned results as suggesting MCC and MCC-LG spectral data sets are three–dimensional, we still evaluate them using both 3 and 4 basis function factorization for the purposes of comparatively assess differences and similarities that may arise due to factorization with a higher rank for the tested sets.

Moreover, we compute a four basis function decomposition for LG because her photopigment opsin genotype confers a potential for expressing four distinct classes of retinal photopigments, and suggests that four distinct signals could arise in LG at the retina level. To cross-check validity of our procedures, we also compute a four basis function decomposition for the MCC because we expect to verify that four–bases do not work equally well for the MCC case, which was developed assuming a trivariant model of color processing. Carrying out decompositions using 4 basis functions for all three test cases allows us to show the procedures we use distinguish between the cases we consider, and permits a means of evaluating the dimensional assumptions on which the design of the MCC and a standard trichromat observer model are based.

For the MCC spectra basis functions were calculated (Fig. 6). Calculated basis functions were normalized twice. NMF can produce ambiguous solutions with respect to factors $\boldsymbol{W}$ and $\boldsymbol{H}$. To avoid this problem, we divided all elements in each column of $\boldsymbol{W}$ by their sum. After that we normalized all basis functions to make their total maximum equal unity.

We compare the basis MCC functions with color matching and cone curves. The correspondence between the color matching functions and basis functions optimized in spectral space and color space is rather good (Fig. 6). Apart from the L-cone, the correspondence to cone fundamentals is also good. Most of basis functions are bell-shaped like color matching or cone curves. The MCC basis functions based on optimization in a color space, are for the most part, more accurate than those optimized in a spectral space (Fig. 6 and Table 1). They are better correlated with matching curves and cone fundamentals. In addition, visual inspection suggests they correspond more closely in shape and sharp modes for the middle and short wavelength curves. The long wavelength curve is not so accurate and gives only rough representation for the range of wavelengths. Therefore correlation coefficients are not given for cone fundamentals for long wavelengths.

In general the correspondence between optimization results and color matching functions is good for the middle range of wavelengths and for the short wavelengths and not accurate for the long wavelengths. This suggests that if, as modeled in the literature [21], the optimization for the MCC set gives rise to a good trichromat result, in the sense that it captures three bases resembling those used in the original MCC model. Next we extend our measurements, expecting a similar generalization when used as optimization procedures for potential tetrachromat spectral sets, and investigate the derived bases that best capture the potential tetrachromat participant's data.

Table 1. Correlation coefficients between color matching functions and cone fundamentals and basis functions optimized in spectral and color spaces.

Color matching functions			
Wavelengths	long	medium	short
Spectral space	0.10	0.99	0.83
Color space	0.16	0.95	0.90
Cone fundamentals			
Wavelengths	long	medium	short
Spectral space	—	0.97	0.89
Color space	—	0.98	0.91

In the next investigations we will employ the simulated spectra measured using painted color patches by potential tetrachromats (Fig. 8 and Fig. 9), where spectral curves are depicted as dashed (CA) or dot-dashed (LG) lines. To give a general representation about color corresponding to each curve we place a related colored patch above each curve's peak.

Consistent with earlier observations, results obtained in spectral space are not as impressive as those obtained using color space optimization (Fig. 8 and Fig. 9). Moreover, the basis functions obtained using spectral optimization and corresponding to red, green and blue colors are less orthogonal. However, the curves behave similar to color space curves.

The optimization results in color space for three basis functions (Fig. 9a and c) are rather close to the MCC test (Fig. 6d). In case these methods suggested that MCC was also characterizable with greater than three–dimensions, we conducted analogous investigations assuming that the MCC is four–dimensional. The results differentiate four CA and LG tetrachromat basis functions (Fig. 9b and d) from four MCC basis functions (Fig. 9e). In this case there is a correspondence only between curves similar to trichromatic curves while the fourth curves are different. For simulated spectra the fourth curve locates in the subrange corresponding to yellow color while the fourth curve of the MCC spectra locates in the subrange corresponding to bluish green (or cyan) color. The four basis functions for CA and LG are similar (Fig. 9b and d)), and, interestingly, coincide with the approximate spectral location where the sensitivity peak of the putative fourth photopigment class is predicted to occur given the L-opsin codon-180 heterozygosity that both observers possess [15, 16].

Following a perceptual learning rationale, it is perhaps not unexpected that despite LG's tetrachromat genotype,

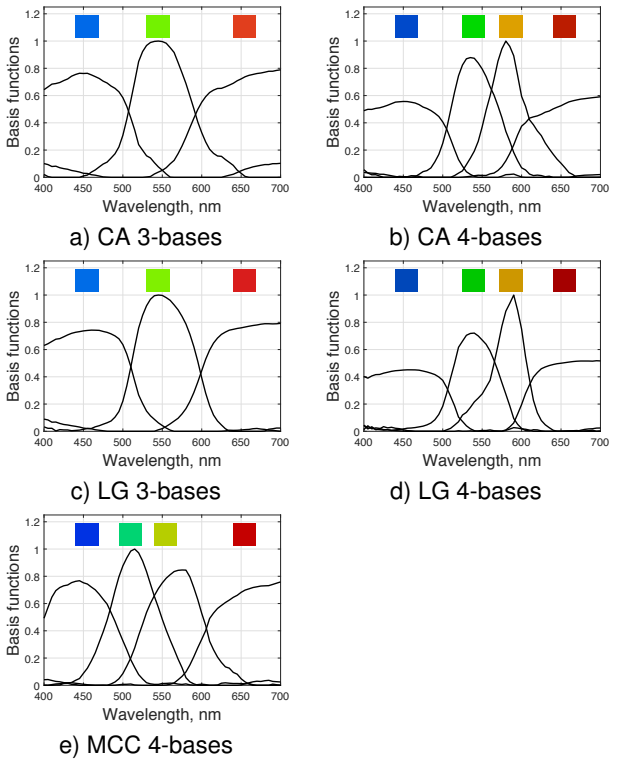

Figure 8. *Optimization in spectral space. The normalized basis functions calculated using the MCC spectra and the simulated tetrachromatic spectra. a) Three basis functions (CA). b) Four basis functions (CA). c) Three basis functions (LG). d) Four basis functions (LG). e) Four basis functions (MCC).*

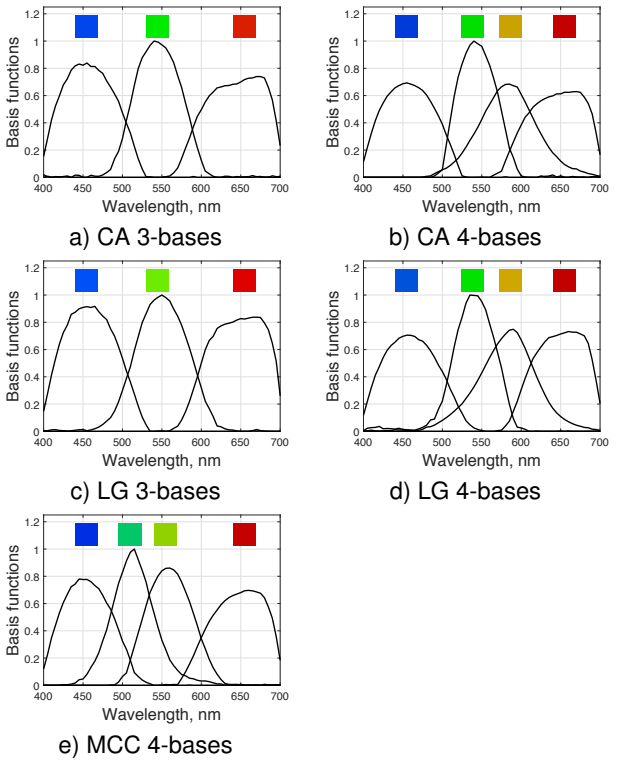

Figure 9. *Optimization in color space. Normalized basis functions calculated using the MCC spectra and two sets of simulated tetrachromatic spectra. a) Three basis functions (CA). b) Four basis functions (CA). c) Three basis functions (LG). d) Four basis functions (LG). e) Four basis functions (MCC).*

her spectral data set is modeled by 3–dimensions (as shown in the ISOMAP results) with by 3– or 4–basis functions. That is, in view of what has been suggested elsewhere concerning the need for perceptual learning in order to realize functional (i.e., dimensional) tetrachromacy [16], it is may not be a surprise that part–time artist LG — who while a skilled artist does not have the extensive longitudinal exposure and continued daily immersion using color appearance judgments when compared to CA who is a full-time professional artist — shows evidence of an extra basis that actually concurs with her genotype, but who does not show as significant of a dimensional deviation (based on the ISOMAP results) as CA who previously was found to empirically exhibit deviations from normal trichromat color vision compatible with dimensionally richer color experience. This pattern of results for LG and CA is consistent with widely–observed finding that individuals with the genetic potential for tetrachromacy frequently do not empirically exhibit functional tetrachromacy. While the idea is currently conjecture, presumably this is due to the plausible scenario that in addition to a genetic potential, exceptional training and perceptual learning is needed to realize functional human tetrachromacy, and, in the absence of a lifetime of color training and practice, many individuals with tetrachromat genotypes, who also express four distinct retinal photopigment classes, may still be found to exhibit normal three-dimensional color vision.

We interpret this result to suggest that the potential tetrachromat CA most likely has four different photoreceptors with response sensitivity characteristics that are approximated by the calculated curves (Fig. 9b). The fourth basis function peaks between the long-wavelength and middle-wavelength basis functions while the remaining functions are close to the basis functions of a trichromat. This is in agreement with what is known from participant CA's photopigment opsin genotype [15, 16], and is consistent with the simulated cone fundamental results found in other investigations of potential tetrachromats [18]. The simulated cone fundamentals derived here for potential tetrachromat CA contain a fourth spectral sensitivity curve located between spectral curves of M-cone and L-cone while the others curves correspond to the Smith-Pokorny cone fundamentals for S-, M- and L-cone classes. Previous empirical results for CA also support the existence of an additional factor in the spectra region corresponding to the four basis function here, that was found to influence (and differentiate from trichromat control participants) CA's perception of color in minimum-motion isoluminance settings. [15, 16]

Note, these findings agree with earlier results for CA from minimum-motion at isoluminance tasks. [15, 16] That is, comparisons of individual's isoluminance settings found CA's results to differ markedly in some regions of color space compared to normal trichromat controls. Jameson

and colleagues [15, 16] report that the comparative sensitivity found in CA's settings suggest she is expressing a fourth cone class (presumed to be a long-wavelength sensitive cone class variant, based on her genotype) which is contributing to cues used to establish isoluminance equilibria, in addition to the usual signal contributions from M-, L- and S-cones that normal trichromats possess. Moreover, the present basis function estimation results also concur with Jameson and colleagues [15, 16] findings that CA's greatest deviations from normal trichromat controls are found for stimuli comprised of dominant wavelengths components from regions between the standard normal M- and L-cone peaks – or, the spectral region where her putative fourth cone class is expected to be most sensitive based on her X-linked opsin genotype. Both sets of results for CA suggest that she possesses a potential tetrachromat genotype that when phenotypically expressed permits richer color experience compared to trichromat controls. [12, 13]

6 Conclusions

We investigated spectral reflectance measurements of color stimuli corresponding to MCC color patches as compared to analogous measures of color patches reproduced through painting by two potential tetrachromat artists. The sets of reflectance measurements show interpretable differences between simulated spectra and MCC spectra in different subranges of wavelengths. Measurement of achromatic spectra sets additionally indicate that consistent with existing results, one potential tetrachromat (CA) has enhanced sensitivity to chromatic content inherent in otherwise dark achromatic, or gray, appearances.

We empirically derived color processing basis functions from the data of two potential tetrachromats (CA and LG). Based on our findings, and consistent with existing psychophysical and opsin genetics research, we suggest that three of the four basis functions derived resemble three basis functions similar to those typically seen in models of standard normal trichromat color vision, while the fourth basis function — in accord with these participants' opsin genotypes and predictions from the photopigment opsin genetics literature — shows a response with peak sensitivity between the response curves corresponding to the normal trichromat medium- and long-wavelength sensitive response curves.

We also showed that when applied to MacBeth Color Checker (MCC) spectral data, the optimization procedures which identified four basis functions for our potential tetrachromats, accurately identified three bases that are consistent with the MCC's underlying trichromat model, implying that the MCC data set was optimized by three basis functions, not four. This latter result gives additional confidence that the optimization procedure is tracking color processing dimensions present in the data sets.

Moreover, when defining the data dimensions inherent in the three sets of spectra (MCC, CA, and LG) we found that spectra from the trichromat model (MCC) was best fit by a three-dimensional color appearance model. This result also gives us confidence in our methods because it suggests that the MCC dimensionality is confirmed as a trichromat model.

By comparison, the dimensionality inherent in the empirically reproduced spectra varied across the two potential tetrachromat participants. That is, the spectral measurements from one potential tetrachromat individual (LG) was best fit by a three-dimensional model, whereas the measured spectra from CA was best fit by a four-dimensional model.

This latter results implies that LG provided color appearance data best modeled by three dimensions, whereas CA provided data best modeled by four dimensions of color experience, and suggests that our procedures are possibly sensitive to perceptual learning effects that might differentiate our two potential tetrachromats. [15, 16]

Future investigations aim to develop a four–channel color processing system with spectral characteristics similar to tetrachromatic basis functions.

Acknowledgements

Portions of these findings were presented at the *Progress in Colour Studies (PICS)* conference, September 2016, University College London, London, UK. This work was funded inpart by the National Science Foundation (#SMA-1416907). Views and opinions expressed in this work are those of the authors and do not necessarily reflect the official policy or position of any agency of the University of California or the National Science Foundation. The authors appreciate and acknowledge assistance provided by Prof. M. Cristina Kenney and Shari Atilano with opsin genotyping of participants. Authors greatly appreciate assistance provided by Prof. Yoichi Miyake, Tokyo Polytechnic University, on spectral measurements and implementing the multispectral technique and Dr. Petri Välisuo's, University of Vaasa, assistance with spectral measurements. Thanks to Dr. Tim Satalich, Institute for Mathematical Behavioral Sciences at UC Irvine, who provided code and assistance with spectral measurements; and to Dr. Ragnar Steingrimsson for valuable feedback on theoretical underpinnings of plausible perceptual processing mechanisms.

References

[1] A. Andriyashin, Non-negative bases in spectral image archiving, Ph.D. Thesis, University of Eastern Finland, Joensuu, Finland, 2011.

[2] S. Atilano, K. A. Jameson and M. Cristina Kenney, Procedures for characterizing the genetic sequences underlying human visual phenotypes: Genotyping methods and a case-study demonstration. *Technical Report Series # MBS 17-04. Institute for Mathematical Behavioral Sciences University of California at Irvine*. Irvine, CA, USA. Available at http://www.imbs.uci.edu/research/MBS%2017-04.pdf.

[3] D. Bimler, J. Kirkland, J. and K. A. Jameson, Quantifying Variations in Personal Color Spaces: Are there Sex Differences in Color Vision? COLOR Research & Application, 29(2), 128-134. 2004.

[4] D. Bimler and J. Kirkland, Colour–space distortion in women who are heterozygous for colour deficiency. Vision Res. **49**, 536–543, 2009.

[5] V. A. Bochko, K. A. Jameson, T. Nakaguchi, Y. Miyake, and J. T. Alander, *Non-negative matrix factorization using genetic algo-*

rithm for spectral colors: ***Substantially Updated Version***. *Technical Report Series # MBS 17-03. Institute for Mathematical Behavioral Sciences University of California at Irvine*. Irvine, CA, USA. Available at http://www.imbs.uci.edu/research/MBS%2016-03.pdf.

[6] Colorimetry, C. I. E. (1986). Publication CIE No. 15.2. Vienna: Central Bureau of the Commission Internationale de L'Eclairage.

[7] Colorlab Toolbox for Matlab by the University of Joensuu Color Group (http://spectral.joensuu.fi)

[8] D. H. Foster, K. Amano, S. M. Nascimento, and M. J. Foster. (2007). The Frequency of Metamerism in Natural Scenes. Optics and Photonics News, 18(12), 47–47.

[9] http://www.gtilite.com/products/color-viewing-lamps/.

[10] B. Hill, High quality color image reproduction: The multispectral solution, The Ninth International Symposium on Multispectral Color Science and Application, IS&T, USA, pp. 1-7, 2007.

[11] S.M. Hood, J. D. Mollon, L. Purves and G. Jordan, Color discrimination in carriers of color deficiency. Vision Research, 46, 2894–2900, 2006.

[12] K. A. Jameson, Highnote, S. M., and Wasserman, L. M., Richer color experience in observers with multiple photopigment opsin genes. Psychonom. Bull. Rev. **8**, 244–261, 2001.

[13] K. A. Jameson, D. Bimler and L. M. Wasserman, Re–assessing Perceptual Diagnostics for Observers with Diverse Retinal Photopigment Genotypes. In *Progress in Colour Studies 2: Cognition*, N. J. Pitchford and C. P. Biggam, eds. (John Benjamins Publishing Co.), pp. 13–33, 2006.

[14] K. A. Jameson, Tetrachromatic Color Vision. Invited contribution to The Oxford Companion to Consciousness. Wilken, P., Bayne, T. & Cleeremans, A. (Ed.s). Pp. 155-158. Oxford University Press: Oxford. 2009.

[15] K. A. Jameson, A. D. Winkler, C. Herrera and K. Goldfarb, The Veridicality of Color: A case study of potential human tetrachromacy, GLIMPSE Journal, 12, 2015.

[16] K. A. Jameson, A. D. Winkler and K. Goldfarb, Art, interpersonal comparisons of color experience, and potential tetrachromacy, Society for Imaging Science and Technology, DOI: 10.2352/ISSN.2470-1173.2016.16HVEI-145, 2016.

[17] G. Jordan and J. D. Mollon, A study of women hererozygous for colour deficiencies. Vision Res. **33**, 1495–1508, 1993.

[18] G. Jordan, Deeb, S. S., Bosten, J. M., and Mollon, J. D. , The dimensionality of color vision in carriers of anomalous trichromacy. Journal of Vision, 10(8), 12-12, 2010.

[19] A. Kaarna, K. Tamura, S. Nakauchi, J. Parkkinen, Non-Negative Bases for Spectral Color Sets, Proc. IMQA, pp. 333-343, 2007.

[20] Macbeth Color Checker Classic. Professional Camera Calibration Target. Manufactured by X-rite for Munsell Color. January 2014 Edition. xritephoto.com

[21] C. S. McCamy, H. Marcus, and J. G. Davidson (1976). "A Color-Rendition Chart". Journal of Applied Photographic Engineering 2(3). 95?99.

[22] J. D. Mollon, "Tho'she kneel'd in that place where they grew?" The uses and origins of primate colour vision. Journal of Experimental Biology, 146.1, 21-38, 1989.

[23] J. D. Mollon, Worlds of Difference. Nature 356, 378-379, 1992.

[24] A.L. Nagy, MacLeod, D.I.A., Heyneman, N.E. and A. Eisner, Four cone pigments in women heterozygous for color deficiency. Journal of the Optical Society of America A 71, 719–722, 1981.

[25] B. Sayim, K. A. Jameson, N. Alvarado and M. K. Szeszel, "Semantic and Perceptual Representations of Color: Evidence of a Shared Color–Naming Function." J. Cogn. Culture **5**, 427–486 (2005).

[26] Wasserman, L. M., Szeszel, M. K. & Jameson, K. A. (2009). Long-Range Polymerase Chain Reaction Analysis for Specifying Photopigment Opsin Gene Polymorphisms. *Technical Report Series # MBS 09-07. Institute for Mathematical Behavioral Sciences University of California at Irvine*. Irvine, CA, USA. Available at http://www.imbs.uci.edu/tr/abs/2009/mbs_09-07.pdf.

[27] J. B. Tenenbaum, V. de Silva, and J. C. Langford, A global geometric framework for nonlinear dimensionality reduction, Science Vol. 290 (5500), pp. 2319-2323, 2000.

[28] H. Qiao, New SVD based initialization strategy for non-negative matrix factorization, Pattern Recognition Letters, Vol. 63, pp. 71-77, 2015.

[29] T. Smith and J. Guild, The C.I.E. colorimetric standards and their use. Transactions of the Optical Society. 33 (3): 73–134. doi:10.1088/1475-4878/33/3/301, 1931-1932.

[30] V. C. Smith and J. Pokorny, Spectral sensitivity of the foveal cone photopigments between 400 and 500 nm. Vision Research, 15, 161–171, 1975.